Leadership in Sustainable Infrastructure
Leadership en Infrastructures Durables

Vancouver, Canada
May 31 – June 3, 2017/ *Mai 31 – Juin 3, 2017*

ELECTRICAL RESISTIVITY RESPONSES OF YOUNG NORMAL STRENGTH CONCRETE MIXES UNDER TEMPERATURE CYCLING

Tomlinson, Douglas G.[1,2]
[1] University of Alberta, Canada
[2] dtomlins@ualberta.ca

Abstract: There is desire within the construction industry for a simple but accurate method of estimating the real-time strength of cast-in-place concrete during curing. Knowing this strength will allow for more rapid construction since formwork removal, post-tensioning, and finishing can be performed earlier and with higher confidence than with existing methods. Electrical resistivity has been proposed as a means of predicting strength but the resistivity of concrete subject to early freezing is not well understood. The electrical resistivity responses of five concrete mixes used in the Ottawa area over 28 days were studied. These mixes had varying water-cement ratios (0.37 to 0.62) and slag replacement values (0 to 28%). The mixes were thermally cycled at 1°C/hr from +24 to -24°C after either 1 or 14 days of room temperature curing. Resistivity increased according to Arrhenius Law as temperature decreased. However, ice formation, which occurred between 0 and -10°C, caused a sudden increase in resistivity that no longer followed Arrhenius Law. A method of using resistivity to estimate the ice formation temperature (datum temperature) is presented that requires considerably less effort than existing techniques. The datum temperature decreases as concrete ages and as slag percentage increases. Resistivity increased as water-cement ratio decreased and is proportional to concrete strength. However, resistivity also increased as slag percentage increased; this is attributed to the slower-reacting slag reducing ion mobility in the concrete. These results indicate that resistivity can be normalized based on temperature and slag percentage to predict the real time strength of cast-in-place concrete.

1 INTRODUCTION

Cast-in-place concrete is common in construction as it is relatively cheap, versatile, and widely available. However, cast-in-place concrete is particularly susceptible to environmental conditions (e.g. temperature, humidity) during curing and this means that its in-place strength is often unknown. Since the in-place strength of concrete is unknown, strength-sensitive construction events (e.g. formwork removal, finishing, or post tensioning) are only planned once there is confidence that the concrete has reached the designed strength and developing this confidence can cause construction delays. Knowing the real-time strength of cast-in-place strength of concrete is advantageous as construction schedules could be accelerated since form stripping or post-tensioning can be performed on a tighter schedule and with better confidence.

Currently, engineers can estimate the strength of cast-in-place concrete cured at temperatures reflecting exterior construction using ASTM C1074-11's maturity method (ASTM 2011). This method is based on developing a baseline strength development curve for concrete cured at a reference temperature (often 25 °C) then using a maturity factor to evaluate the equivalent age for a concrete cured at temperatures differing from the baseline curve. The maturity factor is evaluated using the temperature of the curing concrete and a 'datum temperature', which is the temperature in which concrete strength development is assumed to cease due to ice formation in the mix. This datum temperature can be evaluated experimentally for a mix design using ASTM C1074-11 and is generally between -10 °C and 0 °C in typical concrete mixes (ASTM 2011). Though relatively commonly used in practice, the maturity method does not consider the impact of concrete curing temperature on its long term strength (Charmchi 2015).

Electrical resistivity has been proposed as an alternative method for estimating the strength of cast-in-place concrete in real time. As concrete cures, ion mobility within the mix decreases as pore water reacts with the cement paste. The increase in resistivity over time has been shown to be proportional to the concrete's strength development curve (Whittington et al. 1981). Resistivity has also been shown to be proportional to concrete strength in typical Ordinary Portland Cement (OPC) concrete mixes (Whittington et al. 1981). However, resistivity is also affected by temperature, aggregate type, and the presence of Supplementary Cementitious Materials (SCM) in concrete (Sellehi 2015, Liu and Presuel-Moreno 2014a, Liu and Presuel-Moreno 2014b). With regard to temperature, resistivity changes according to the Arrhenius relationship (Equation 1); this has been shown to apply to concrete cured at temperatures between 10 °C to 45 °C (Liu and Presuel-Moreno 2014a).

[1] $\rho_t = \rho_0 \times e^{\left[\frac{E_a}{R}\left(\frac{1}{T}-\frac{1}{T_0}\right)\right]}$

Where ρ_t is the measured resistivity at a temperature, T (K). E_a is the concrete mix activation energy, R is the gas constant, T_0 is the reference temperature (K), and ρ_0 is the resistivity at the reference temperature, T_0 (K). This relationship has also been shown to hold true for mortar cubes until ice formation begins at some point between 0 °C and -10 °C (Farnam et al. 2015, Sato and Beauduin 2011). The reason ice formation occurs at temperatures below 0 °C is attributed to the presence of ions in the pore solution causing a freezing point depression (Liu and Presuel-Moreno 2014a). Ice formation begins in the largest pores then continues into smaller pores as the temperature continues to decrease (Zuber et al. 2000). Aggregates also affect resistivity readings and indicate that concrete mixes should be investigated in addition to mortar tests (Sellehi 2015, Liu and Presuel-Moreno 2014b).

SCMs enhance the long term performance of concrete and have the added benefit of reducing the embodied energy of a concrete mix. Though beneficial in the long term, SCMs (particularly ground granulated blast furnace slag (GGBS) and fly ash) are slower reacting than cement and lead to lower strength concrete during its early life (<60 days) than an OPC concrete mix (Liu and Presuel-Moreno 2014b). The fact that SCM are slower reacting leads to lower ion mobility in the mix and thus higher resistivities than OPC mixes with the same final strength. This effect is most prominent with GGBS followed by fly ash and then silica fume (Sellehi 2015).

This paper discusses the resistivity change in five normal strength concrete mixes cooled from +24 °C to -24 °C after either 1 or 14 days of curing. The mixes include both OPC mixes and ground granulated blast furnace slag (GGBS) blended mixes. The resistivity readings are also compared to the 28-day compressive strengths of the mixes to better understand how resistivity and concrete strength are related in normal strength concrete mixes batched with and without SCMs.

2 EXPERIMENTAL PROGRAM

2.1 Mix Designs

Five normal strength concrete mixes currently used by contractors in the Ottawa area were considered in this study. The mix designs are shown in Table 1. Three mixes (O1, O2, and O3) used Type GU (general use) cement as the sole binding agent while the remaining two mixes (S1 and S2) used GGBS as a SCM. Rounded limestone with a nominal maximum aggregate size of 12 mm was used as the coarse aggregate in all mixes; sand was used as the fine aggregate.

Mix O1 was designed as a baseline mix with a water cementitious materials (w/cm) ratio of 0.41. Mixes O2 and O3 contained higher w/cm ratios (0.54 and 0.62 respectively). Mixes S1 and S2 were designed to have similar w/cm ratios as O1 but with 18 and 28% of the cement replaced with GGBS.

Table 1: Mix designs considered in this study

Mix Design	O1	O2	O3	S1	S2
Cement, kg/m^3	365	280	265	333	298
Granulated Ground Blast Furnace Slag (GGBS), kg/m^3	0	0	0	77	117
Water, kg/m^3	150	150	165	153	155
Coarse Aggregate, kg/m^3	1075	1055	1055	1080	1070
Fine Aggregate, kg/m^3	750	860	940	680	815
w/cm ratio	0.41	0.54	0.62	0.37	0.37

2.2 Procedure

Each mix was batched using a 0.15 m^3 capacity concrete drum mixer and cast into five 102 mm diameter concrete cylinder molds. Three of these cylinders were capped and cured at room temperature then tested in accordance with ASTM C39-15a (ASTM 2015) after 28 days. The remaining two cylinders from each batch were fitted with the monitoring system described in the following section. The first monitored cylinder was put into an environmental conditioning chamber after 1 day while the second monitored cylinder was put into the conditioning room after 14 days. Once in the chamber, the cylinders were thermally cycled from +24 °C to -24 °C twice at a rate of 1 °C/hr, following the process illustrated in Figure 1. The first cooling period forms the basis behind a large part of the results and discussion section and is highlighted in Figure 1 as the region of interest for this study. After cycling was complete, the cylinders were removed from the environmental chamber and left to cure at room temperature.

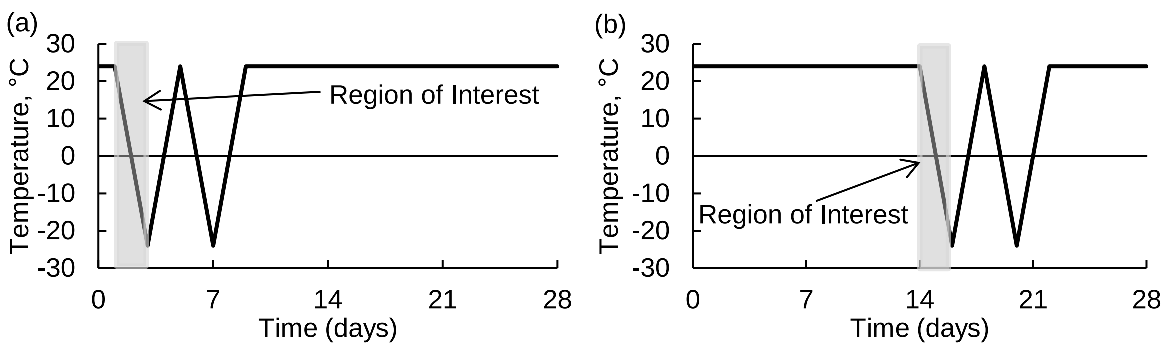

Figure 1: Temperature cycling periods for (a) 1 day and (b) 14 day starting points

2.3 Instrumentation

The monitoring system consists of a case that contains a power supply, a data logger, a temperature sensor, and two mounts for threaded steel rods that act as electrodes (Figure 2). The electrodes were inserted through a cylinder cap and connected to the monitoring system. After concrete was cast into the cylinder mold, the electrodes and temperature sensor were inserted into the still-wet concrete. The cylinder was then vibrated by hand to ensure that the electrodes were not surrounded by voids. The cylinder was capped and the data logging was started. During the first day of curing and during temperature cycling, data (i.e. temperature and electrical resistance) was recorded at 15 minute intervals; during all other periods data was collected at 60 minute intervals.

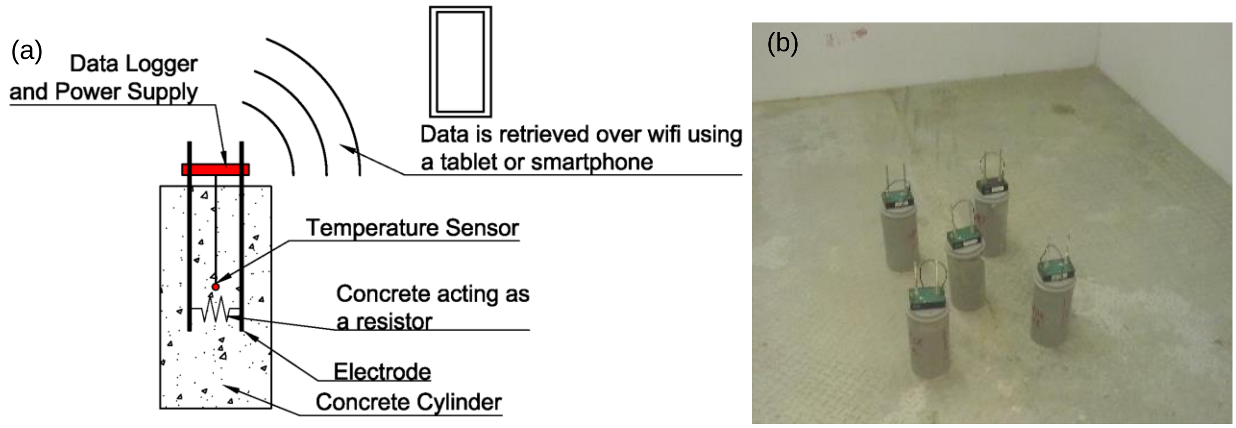

Figure 2: Instrumentation system showing (a) schematic of sensor (b) cylinders with sensors in environmental chamber.

In order to determine resistivity, the geometry factor, *k*, for the cylinder mold was needed. The geometry factor was found to be $9.13m^{-1}$ using a calibration solution with a known resistivity. Using *k*, resistivity, ρ, could then be calculated from the electrical resistance reading, *R*, using Equation 2.

[2] $\rho = R/k$

3 RESULTS AND DISCUSSION

3.1 Resistivity-Temperature Relationships

The effect of temperature on electrical resistivity for the first cooling cycle from each mix is shown in Figure 3. As temperature decreased, resistivity increased for each mix. With the exception of the older GGBS mixes at 14 days (S1 and S2), the resistivity-temperature relationship follows the Arrhenius Law given in Equation 1 until the onset of ice formation at some point between 0 °C and -10 °C. Ice is a poor conductor of electricity and severely limits ion flow in the mix; the onset of ice formation is represented by a sudden increase in resistivity. Once ice formation began, the resistivity-temperature relationships for each mix became linear and increased at a considerably faster rate as temperatures continued to decrease.

The same general trends were observed in both the 1 and 14-day cooling cycles (with the exception of S1 and S2 which will be discussed later). The concrete resistivity after 14 days of curing was higher than those of the mixes after 1 day of curing at temperatures above the phase transition temperature (onset of ice formation). This is due to the 14 day old mixes having less available pore water to carry a current. This causes a reduction in ion mobility and thus an increase in resistivity. However, after the onset of ice formation, the resistivity of the 14 day old mixes was actually slightly lower than the 1 day old mixes. Less ice formed in the older mixes since there is less available pore water; the reduction in ice formation also caused a decrease in resistivity compared to the younger mixes with more pore water available to turn into ice.

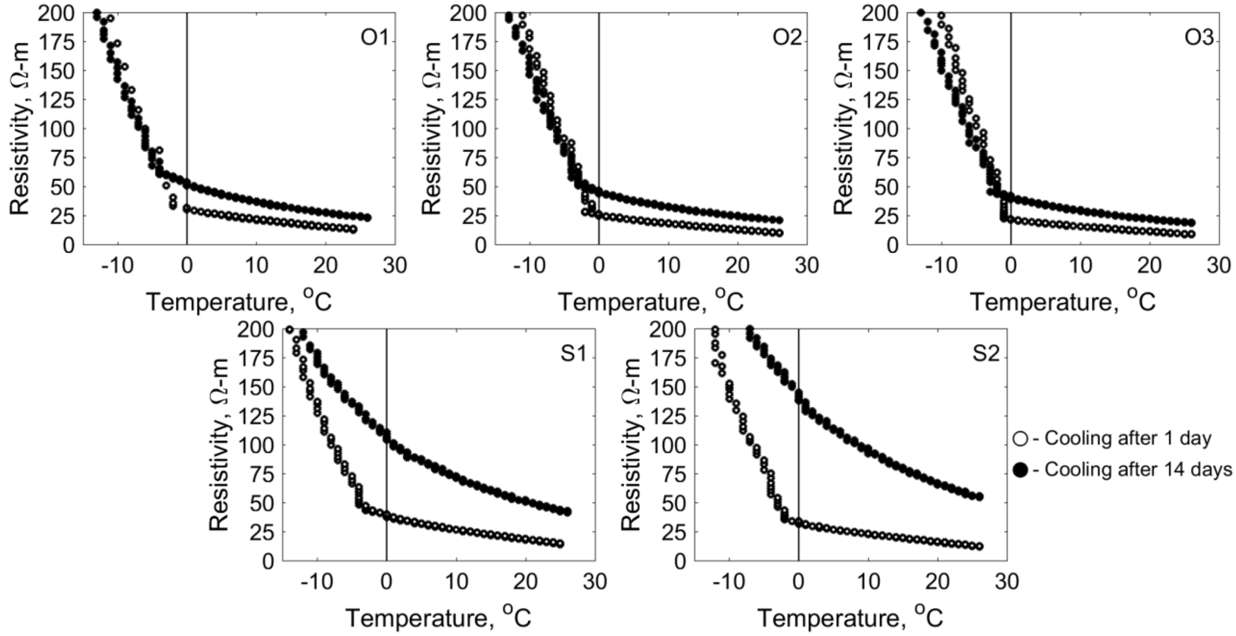

Figure 3: Resistivity versus temperature readings during cylinder cooling for each mix

3.2 Phase Transition Temperature

The phase transition point where ice formation begins is believed to coincide with its datum temperature and that strength development is expected to cease in concrete cured at temperatures below this point. Currently, the datum temperature is determined using mortar cubes and requires a detailed experimental process that takes a month or longer to complete and for one mix design (ASTM 2011). It is suggested to use the following process using resistivity to simplify the task of determining the concrete datum temperature:

1. Cast a concrete mix and fit it with the monitoring system so its resistivity can be tracked.
2. Freeze the concrete after a desired curing period (in this case, 1 and 14 days) to establish its temperature-resistivity curve.
3. Use curve fitting software to fit two curves and then evaluate the point of intersection. The first curve would fit the Arrhenius relationship and use data from between 5 °C and 25 °C, the second curve would be a linear relationship fitting the data between -10 °C and -20 °C. The temperature at the point of intersection would then be used as the datum temperature for the concrete mix.

This process was used to evaluate the phase transition point for each mix at both the 1 and 14-day cooling periods; these results are shown in Table 2.

Table 2: Phase transition point for each mix and cooling time

Mix	1 day Phase Transition Temperature, °C	14 day Phase Transition Temperature, °C
O1	-2.6	-4.6
O2	-2.7	-4.1
O3	-1.7	-3.4
S1	-4.8	-8.5
S2	-3.6	-7.5

In Table 2, it can be seen that the transition temperature decreases as the mix ages. Ice formation begins in the largest pores then progresses to smaller pores as the temperature decreases further (Zuber et al. 2000). Since there is less water available to carry current in older concretes, the water no longer occupies the largest pores. This leads to the remaining pores being smaller and causing a reduction in the ice formation temperature.

The transition temperature also was lower in the GGBS mixes than the OPC mixes. The reasoning behind this needs further study since GGBS reacts slower than cement (i.e. the freezing point depression caused by ions in the solution should be less severe) and has similar particle sizes to cement (i.e. pore sizes are essentially the same and should not affect the ice formation temperature).

3.3 Water/Cementitious Material Ratio Effect on Resistivity

The effect of the water/cementitious materials ratio on resistivity can be seen in Figure 4. As w/cm ratio increases, the concrete resistivity decreases across all concrete ages investigated. This agrees with previous work (Whittington et al. 1981); this is expected since more water is available in mixes with higher w/cm ratios to transmit ions, causing a loss in resistivity. Similarly, the larger amount of available water increases the mix freezing point (Table 2) as the ions in the pore water are more diluted.

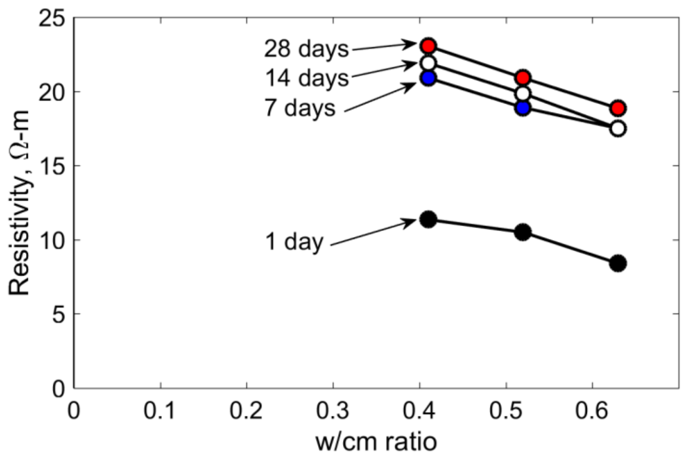

Figure 4: Effect of water cement ratio on resistivity in concrete at various curing dates

3.4 GGBS Effect on Resistivity

The temperature-resistivity relationship trends were very similar for the OPC mixes (O1, O2, and O3) and the blended GGBS mixes (S1 and S2) during the cooling period after 1 day (Figure 5(a)). However, these trends no longer applied to the blended GGBS mixes cooled after 14 days (Figure 5(b)). After 14 days, the blended GGBS mixes have considerably higher resistivities than O1 and the sudden change in resistivity associated with ice formation is not immediately apparent.

The similarities after the first day of curing between O1, S1, and S2 are attributed to the mixes being governed by the cement reaction. However, in the 14-day old mixes the slower reacting GGBS governs the resistivity of the GGBS blended mixes. GGBS reacts at a slower rate than cement and thus has reduced ion mobility (Sallehi 2015); this reduction in ion mobility causes an increase in resistivity that becomes clear after 14 days of curing.

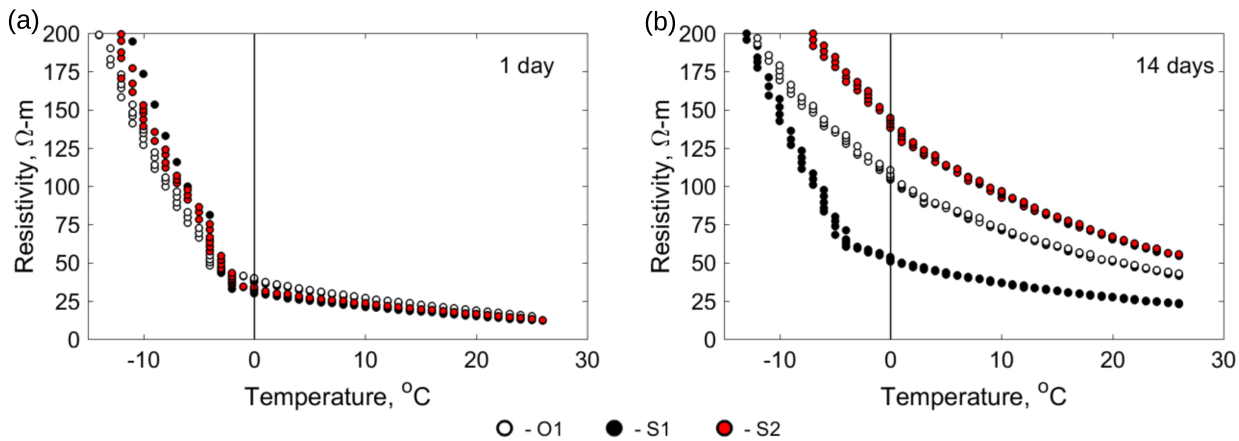

Figure 5: Effect of slag on resistivity-temperature relationships after (a) 1 day and (b) 14 days

The impact of GGBS on resistivity over time is further illustrated in Figure 6. After the first day of curing, there is no significant effect of GGBS on resistivity related to O1. However, after 7 days it becomes clear that the slag mixes have higher resistivities at room temperture than O1. Interestingly, over the investigated GGBS replacement percentages, the increase in resistivity is linear. This indicates that normalizing mix resistivity to account for GGBS replacement percentage may only require a linear adjustment; this relationship should be investigated more in future.

Resistivity in the GGBS mixes also continues to increases substantially after 7 days wheras the OPC mix resistivity increases after 7 days are considerably more modest. For instance, the percentage gain in resistivity in O1 from 7 to 14 days was 5% while it was 26% in S1 and 31% in S2.This is attributed to the GGBS-blended mixes reacting slower than the OPC mixes. After 7 days, the bulk of strength development in OPC mixes has occurred while this has not occurred with the GGBS mixes.

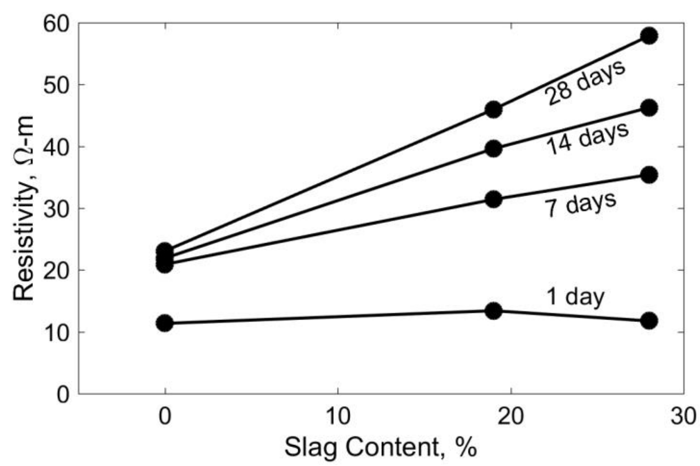

Figure 6: Effect of GGBS replacement percentage on resistivity readings over time.

3.5 Concrete Resistivity and Strength Comparisons

The strength results are summarized in Table 2. With the OPC mixes, strength increased as w/cm ratio decreased, as expected. Similarly, the higher resistivities seen in O1 compared to the lower strength O2 and O3 mixes agree with findings from Whittington et al (1981). For the tested mixes, the ratio of each mix's 28-day strength, f_c', to its final resistivity reading gives similar results for the OPC mixes (ranging between 1.1 and 1.2), showing that resistivity is proportional to compression strength, agreeing with Liu and Presuel-Moreno (2014a). However, mixes S1 and S2 had substantially lower ratios of 0.68 and 0.53 respectively.

This indicates that if someone were to use a baseline strength-resistivity curve for estimating strength that GGBS (or other SCM) blended mixes with would give misleadingly and unconservative results if the SCM contribution is ignored. However, as shown in Figure 7, the change in the strength/resistivity ratio with respect to GGBS percentage is roughly linear for the tested mixes. This relationship should be investigated more in the future to aid in developing general resistivity/strength prediction models for concrete with supplementary cementitious materials such as GGBS, fly ash, or silica fume.

Table 3: Results from strength tests and final resistivity readings

Mix	Mix Strength (f_c'), MPa	Final Resistivity (ρ), Ω-m	f_c'/ρ ratio
O1	25.5±1.5*	22.6	1.13
O2	24.5±0.6	20.3	1.20
O3	20.9±0.7	18.9	1.10
S1	34.1±3.9	50.1	0.68
S2	33.5±2.2	62.7	0.53

*Second value in mix strength readings is the mix standard deviation

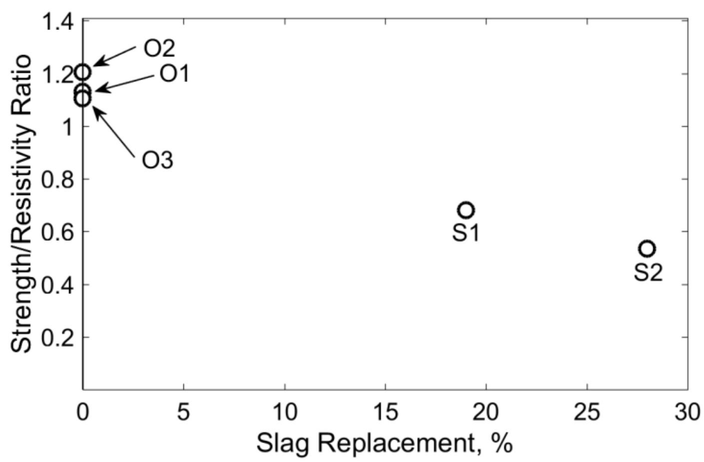

Figure 7: Ratio of slag related to the strength ratio

4 CONCLUSIONS AND RECOMMENDATIONS

The electrical resistivities of five different normal strength concrete mixes with and without granulated ground blast furnace slag as a SCM were monitored during their first month of curing. These mixes were subjected to temperature decreases from +24 to -24 °C after either 1 or 14 days of curing and the resistivity-temperature relationships for each mix were developed and compared to 28-day strength tests. Based on this study, the following was concluded:

1. Resistivity increases as temperature decreases. This relationship follows Arrhenius Law until ice formation begins at which point the change in resistivity with temperature becomes significantly larger and follows a linear trend.
2. Ice formation occurs at temperatures between 0 °C and -10 °C. The temperature of ice formation decreases as the concrete ages and was also found to be lower in GGBS blended mixes.
3. For the tested OPC mixes, resistivity was inversely proportional to water cement ratio and directly proportional to concrete strength. Resistivity was also directly proportional to the percentage of cement that was replaced with GGBS.
4. The blended GGBS mixes behaved similarly to the OPC mixes after the 1 day of curing but they showed considerably higher resistivities than the OPC mixes after 7 days. The effect of GGBS on

resistivity is greater than those of temperature (provided temperatures remain higher than the phase transition temperature) and water/cement ratio.

Based on the results, there is promise in using electrical resistivity to predict the strength of cast in place concrete. However, concrete strength predictions using resistivity readings will need to account for temperature and mix design considerations such as the percentage replacement of cement with SCM. Future work will incorporate cylinders being cured at constant temperatures ranging between -10 °C and +35 °C in order to better understand the relationships between resistivity and curing temperature. These results should then be used to make strength predictions using resistivity and compare those to predictions from the ASTM C1074-11 Maturity Method.

REFERENCES

ASTM International. 2011. ASTM C1074-11: Estimating Concrete Strength by the Maturity Method.

ASTM International. 2015. ASTM C39-15a: Standard Test Method for Compressive Strength of Cylindrical Concrete Specimens.

Charmchi, G. 2015. The Role of Concrete Maturity in Resistivity-Based Performance Specifications. MSc Thesis. University of Toronto, Toronto, ON, Canada.

Farnam, Y., Todak, H., Spragg, R. and Weiss, J. 2015. Electrical Response of Mortar with Different Degrees of Saturation and Deicing Salt Solutions during Freezing and Thawing. *Cement and Concrete Composites*, **59**: 49-59.

Liu, Y. and Presuel-Moreno F.J. 2014a. Normalization of Temperature Effect on Concrete Resistivity by Method Using Arrhenius Law. *ACI Materials Journal*, **111**(4): 433–442.

Liu, Y. and Presuel-Moreno, F.J. 2014b. Effect of Elevated Temperature Curing on Compressive Strength and Electrical Resistivity of Concrete with Fly Ash and Ground-Granulated Blast-Furnace Slag. *ACI Materials Journal*, **111**(5): 531-542.

Sallehi, H. 2015. Characterization of Cement Paste in Fresh State using Electrical Resistivity Technique. MSc Thesis. Carleton University, Ottawa, ON, Canada.

Sato, T. and Beaudoin, J.J. 2011. Coupled AC Impedance and Thermomechanical Analysis of Freezing Phenomena in Cement Paste. *Materials and Structures*, **44**(2): 405-414.

Whittington, H.W., Forde, M.C., and McCarter, J. 1981. The Conduction of Electricity Through Concrete. *Magazine of Concrete Research*, **33**(114): 48-60.

Zuber, B., and Marchand, J. 2000. Modeling the deterioration of hydrated cement systems exposed to frost action - Part 1: Description of the mathematical model. *Cement and Concrete Research*, **30**(12): 1929-1939.